Protein Science (1996), 5:1765–1775. Cambridge University Press. Printed in the USA.

Crystal structure of the 2[4Fe-4S] ferredoxin from *Chromatium vinosum*: Evolutionary and mechanistic inferences for [3/4Fe-4S] ferredoxins

JEAN-MARC MOULIS,[1] LARRY C. SIEKER,[2] KEITH S. WILSON,[3,4] AND ZBIGNIEW DAUTER[3,4]

[1] CEA, Département de Biologie Moléculaire et Structurale, Laboratoire Métalloprotéines, 17 rue des Martyrs, 38054 Grenoble Cedex 9, France
[2] Department of Biological Structures, SM/20, University of Washington, Seattle, Washington 98195
[3] European Molecular Biology Laboratory, Outstation Hamburg, c/o DESY, Notkestrasse 85, 22603 Hamburg, Germany
[4] Department of Chemistry, University of York, Heslington, York YO1 5DD, United Kingdom

(RECEIVED April 25, 1996; ACCEPTED June 28, 1996)

Abstract

The crystal structure of the 2[4Fe-4S] ferredoxin from *Chromatium vinosum* has been solved by molecular replacement using data recorded with synchrotron radiation. The crystals were hexagonal prisms that showed a strong tendency to develop into long tubes. The hexagonal prisms diffracted to 2.1 Å resolution at best, and a structural model for *C. vinosum* ferredoxin has been built with a final R of 19.2%. The N-terminal domain coordinates the two [4Fe-4S] clusters in a fold that is almost identical to that of other known ferredoxins. However, the structure has two unique features. One is a six-residue insertion between two ligands of one cluster forming a two-turn external loop; this short loop changes the conformation of the Cys 40 ligand compared to other ferredoxins and hampers the building of one NH···S H-bond to one of the inorganic sulfurs. The other remarkable structural element is a 3.5-turn α-helix at the C-terminus that covers one side of the same cluster and is linked to the cluster-binding domain by a six-residue external chain segment. The charge distribution is highly asymmetric over the molecule. The structure of *C. vinosum* ferredoxin strongly suggests divergent evolution for bacterial [3/4Fe-4S] ferredoxins from a common ancestral cluster-binding core. The unexpected slow intramolecular electron transfer rate between the clusters in *C. vinosum* ferredoxin, compared to other similar proteins, may be attributed to the unusual electronic properties of one of the clusters arising from localized changes in its vicinity rather than to a global structural rearrangement.

Keywords: *Chromatium vinosum*; crystal structure; electron transfer; evolution; ferredoxin; hydrogen bond; iron-sulfur

Iron-sulfur proteins are increasingly emerging as a complex and diverse class of proteins fulfilling a number of different functions (Cammack, 1992). Ferredoxins with [4Fe-4S] clusters appear to be ubiquitous electron transfer proteins in most anaerobic microorganisms. Two main classes can be distinguished: one includes high-reduction-potential (50–450 mV versus the normal hydrogen electrode or NHE) ferredoxins, which contain only one [4Fe-4S] cluster; the other is composed of a more diverse group of proteins with one or two clusters exhibiting low reduction potentials in the range from −650 to −250 mV. A wealth of structural and spectroscopic data indicate that these two sets of proteins differ by the redox transition of the [4Fe-4S] cluster (Carter et al., 1972; Moulis et al., 1988; Backes et al., 1991).

Reprint requests to: Jean-Marc Moulis, CEA/Grenoble, DBMS-MEP, 17 rue des Martyrs, 38054 Grenoble Cedex 9, France; e-mail moulis@ebron.ceng.cea.fr.

The current discussion is limited to low-potential ferredoxins. To date, only five low-potential [4Fe-4S] ferredoxins have been examined by X-ray crystallography at high resolution, despite the importance of this technique in the understanding of structure-function relations. The 3D crystal structures available in the Protein Data Bank (Bernstein et al., 1977) are of the ferredoxins from *Peptostreptococcus asaccharolyticus* (formerly *Peptococcus aerogenes*, Adman et al., 1973, 1976), *Clostridium acidurici* (Duée et al., 1994), *Bacillus thermoproteolyticus* (Fukuyama et al., 1989), ferredoxin I from *Desulfovibrio africanus* (Séry et al., 1994), and ferredoxin I from *Azotobacter vinelandii* (Stout, 1989). The structure of a related [3Fe-4S] ferredoxin II from *Desulfovibrio gigas* is also known (Kissinger et al., 1991). In addition, structures of *Clostridium pasteurianum* ferredoxin, a close relative of *Clostridium acidurici* ferredoxin, have been derived from NMR data (Bertini et al., 1995). For convenience, the ferredoxins of known structure are listed in Table 1 with the acronyms used throughout the text. The number of 3D structures has to be considered in relation with

Table 1. *3[4Fe-4S] Ferredoxins for which the 3D structure is known*

Acronym	Organism	Reference	PDB code	Method/resolution
Two [4Fe-4S] clusters				
CvFd	*Chromatium vinosum*	Present study	1BLU	X-ray/2.1 Å
PaFd	*Peptostreptococcus asaccharolyticus*	Adman et al. (1976)	1FDX	X-ray/2.0 Å
CaFd	*Clostridium acidurici*	Duée et al. (1994)	1FDN	X-ray/1.84 Å
CpFd	*Clostridium pasteurianum*	Bertini et al. (1995)	1CLF	NMR
One [4Fe-4S] cluster				
BtFd	*Bacillus thermoproteolyticus*	Fukuyama et al. (1989)	2FXB	X-ray/2.3 Å
DaFdI	*Desulfovibrio africanus*	Séry et al. (1994)	1FXR	X-ray/2.3 Å
One [4Fe-4S] plus one [3Fe-4S] cluster				
AvFdI	*Azotobacter vinelandii*	Stout (1989)	1FDD	X-ray/1.9 Å
One [3Fe-4S] cluster				
DgFdII	*Desulfovibrio gigas*	Kissinger et al. (1991)	1FXD	X-ray/1.7 Å

[a] AvFdI and DaFdI refer to the ferredoxin I molecules from these two organisms and DgFdII to the ferredoxin II.

the several tens of such proteins isolated to date (Matsubara & Saeki, 1992).

Of these known structures, CvFd, PaFd, CaFd, and CpFd have two [4Fe-4S] clusters. AvFdI has one [4Fe-4S] cluster and one [3Fe- 4S] cluster. BtFd and DaFdI ferredoxins have a single [4Fe-4S] cluster and DgFdII contains only a [3Fe-4S] cluster. A common feature of these molecules is the very similar geometry of the [4Fe-4S] clusters, which extends to those of high-potential ferredoxins (Carter et al., 1972; Moulis et al., 1988; Backes et al., 1991) and other [4Fe-4S]-containing proteins. The clusters have the shape of a distorted cube, with the Fe and S (inorganic sulfur) atoms at alternative apexes: these atoms form two interpenetrating tetrahedra. Each Fe atom is coordinated by three inorganic sulfurs and by a fourth S atom from a cysteine residue. In view of the common geometry of the [4Fe-4S] clusters in proteins, the polypeptide chain plays a major role in modulating their properties and more 3D structures are needed to understand the means by which the protein matrix influences the function of this type of inorganic cofactor.

The present protein, CvFd, is a case in point. It contains two [4Fe-4S] clusters but has eight amino acids separating two of the cysteines coordinating one of the clusters. This sequence motif is found in ferredoxins isolated from photosynthetic bacteria but not in most other ferredoxins for which the spacing between equivalent cysteines is two amino acids. In addition, the last coordinating cysteine is followed by a C-terminus of 29 amino acids in CvFd; similar segments might only occur in the putative products of a few genes from nonphotosynthetic bacteria. These findings suggest strongly that CvFd could be the prototypical protein of a new family of ferredoxins (Moulis, 1996).

The peculiarities in the primary structure of CvFd may contribute to the very low reduction potential around −500 mV (Smith & Feinberg, 1990) and to the significantly slower rate of intramolecular electron transfer between the two clusters compared to CaFd and CpFd (Huber et al., 1995). It is thus appropriate to extend the structural comparison among the presently available structures of ferredoxins to that of CvFd. We have determined its X-ray structure at 2.1 Å resolution.

Results

Quality of the structure

The Ramachandran plot of backbone torsion angles (ϕ,ψ) is given in Figure 1. There are no residues outside the allowed regions of the plot. The (ϕ,ψ) torsion angles were not restrained during the refinement and provide a good validation of the correctness of the model. The conformation of the peptide bond of Glu 28 was flipped

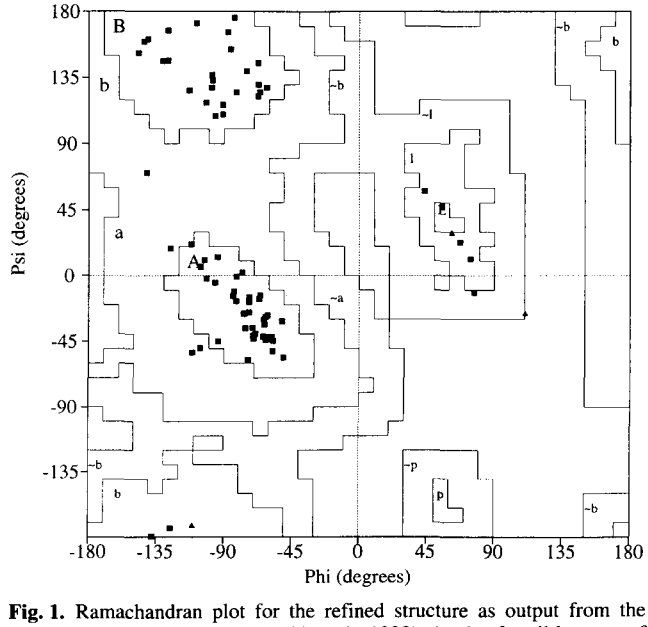

Fig. 1. Ramachandran plot for the refined structure as output from the PROCHECK program (Laskowski et al., 1993). Angles for all but one of the residues lie in the allowed regions and the single outlier (Asp 12) is just on the edge of the left-handed helical region. Glycine residues are shown as triangles.

with respect to its position in the starting model (PDB code 1FDX) on the basis of weak, but visible, electron density and now lies in an accepted region; its position remains poorly defined. The electron density for most of the chain is well defined; regions are shown in Figure 2 for one of the metal clusters and a well-ordered part of the chain.

The Wilson plot (Wilson, 1942) suggests an overall B factor of 21.9 Å^2. The mean B value per residue is plotted as a function of residue number independently for the main chain and side chains in Figure 3. The average B value for the well-ordered main-chain atoms is about 20 Å^2, corresponding to a mean displacement for these atoms from their average position of about 0.5 Å. The parts of the chain showing substantial flexibility are exposed to the surface (Fig. 4). The main chain for two regions on the surface of the molecule (residues 25–29 and 65–70) is particularly ill defined

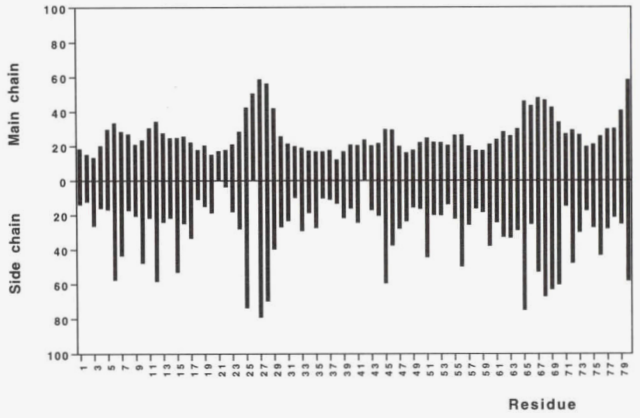

Fig. 3. B-factors (Å^2) for each residue averaged independently for the main chain and for the side-chain atoms.

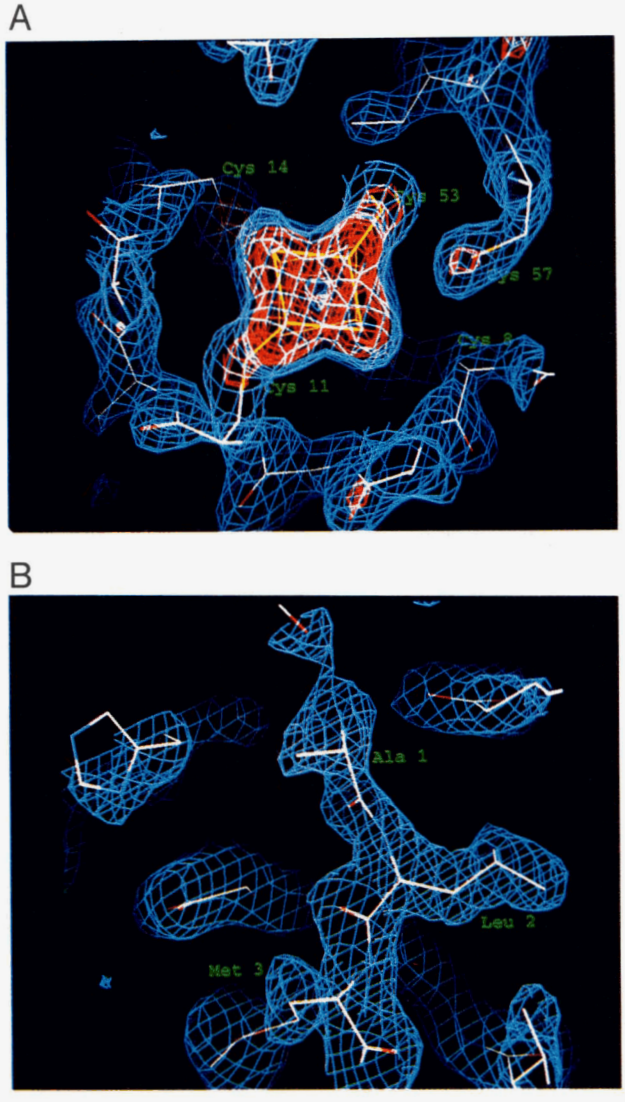

Fig. 2. Representative regions of the ($3F_o - 2F_c$, α_c) electron density map computed with phases from the final model. Maps are contoured at electron density levels of 0.33 e^- (1σ, violet), 0.5 e^- (1.5σ, blue), and 1.5 e^- (4.5σ, red). **A:** Cluster I. Despite the proximity of the cluster, Cys 57 is the only cysteine not coordinating an iron atom. **B:** The density for a well-ordered region of the model including residues 1–3.

and presumed to be flexible. Side chains show even more mobility, with 13 of them having mean B values above 50 Å^2. To put this in context, a B of 50 Å^2 corresponds to a mean atomic displacement of roughly 0.8 Å. The two C-terminal residues could not be located.

Crystal packing

The packing of CvFd molecules in the cell is rather loose (Fig. 5). The cell volume of 181,000 Å^3 and the molecular mass of 9,751 Da (Pétillot et al., 1995) give a V_M of 3.09 Å^3 Da^{-1}, which corresponds to a solvent content of 60.0% (Matthews, 1968). The only direct intermolecular H-bonds are formed between Ile 9 O and two atoms on the molecule related by 3_1 symmetry, Arg 77 NH1 (2.74 Å) and Arg 72 NH2 (3.00 Å). All other H-bonding contacts are mediated by at least one water molecule. CvFd forms no well-defined oligomeric aggregates in the crystal and the monomer is the obvious structural unit, as expected from biochemical data. The loose packing is probably responsible for the relatively poor order in the crystals. Solvent accessibility of the free molecule (5,100 Å^2 in total) and in the crystal lattice (total 4,350 Å^2) is shown as a function of residue number in Figure 4: only 750 Å^2 (15%) are buried by the lattice contacts.

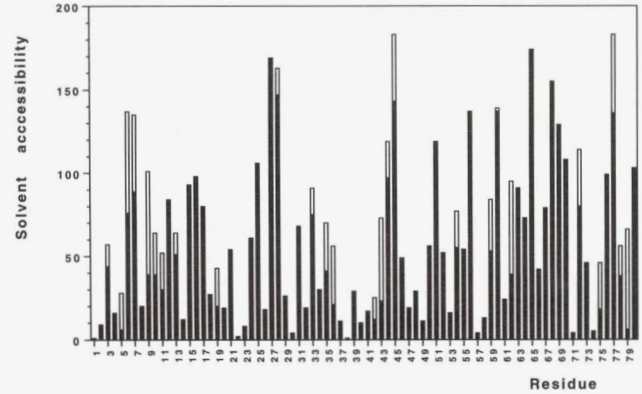

Fig. 4. Accessible surface area (Å^2) for each residue in the crystal lattice (filled bars) and for the molecule isolated from the crystal environment (empty bars).

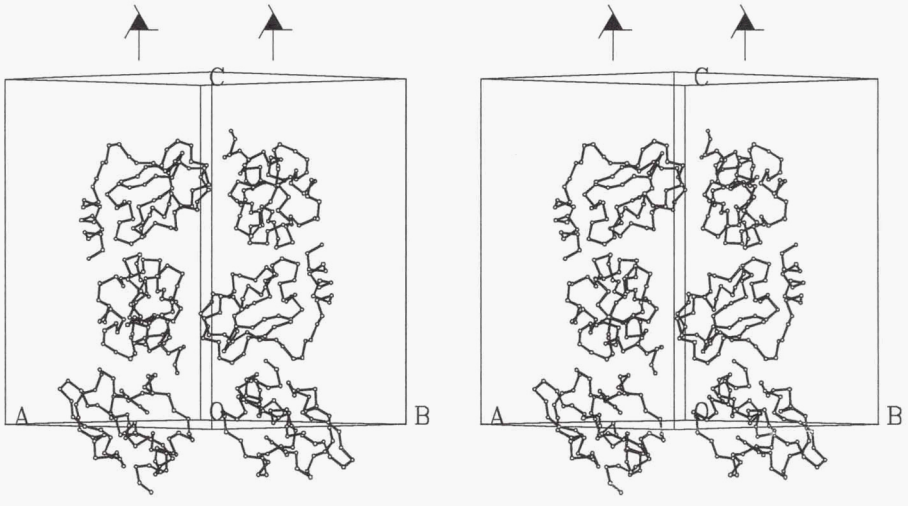

Fig. 5. Stereo view of the packing of CvFd molecules in the crystal viewed perpendicular to the threefold axis.

Solvent structure

As was expected, given the flexibility of the protein itself, the temperature factors were high for the full occupancy 85 water molecules of the model, with an average value of 48 Å^2. All lay on the surface of the protein, with one exception. A single water molecule with low *B* value is buried in the cavity formed between the top of the region enclosing Cluster II and the C-terminal helix. In keeping with previous publications, we define Cluster I as that coordinated by cysteines 8, 11, 14, and 53, and Cluster II by cysteines 18, 37, 40, and 49. The buried water molecule forms three good H-bonds to Thr 38 OG1 (2.67 Å), Val 41 O (2.67 Å), and His 43 ND1 (2.63 Å), all residues that are unique to CvFd, and a single weak one to Asn 20 OD1 (3.54 Å) (Fig. 6 and Kinemage 1). This water molecule may be involved in the stabilization of the structure, particularly in the region of eight amino acids linking two of the ligands of Cluster II.

In the CaFd structure (Duée et al., 1994), four water molecules are involved in forming a pseudo β-sheet with the N- and C-terminal strands. There are water molecules in equivalent positions for three of these in CvFd (Fig. 7 and Kinemage 1).

Description of the fold

A stereo ribbon representation of the polypeptide backbone of CvFd with the two clusters and the charged residues is shown in Figure 8 and Kinemage 1. All basic residues are concentrated in the unique regions of CvFd, and the resulting asymmetry of the charge distribution may be related to the interactions with redox partners if these are electrostatically driven through dipolar contributions (Moulis & Davasse, 1995).

There is essentially no secondary structure in the first 58 residues of the chain, apart from a minimal helix of one turn, residues 47–52, and a short β-sheet between residues 22 and 33. In addition, there is an even shorter sheet made up of residues 1–3 and 59–61. This part of the molecule shows the approximate twofold internal symmetry relating the two clusters and their local environments. The folding of the chain around the two [4Fe-4S] clus-

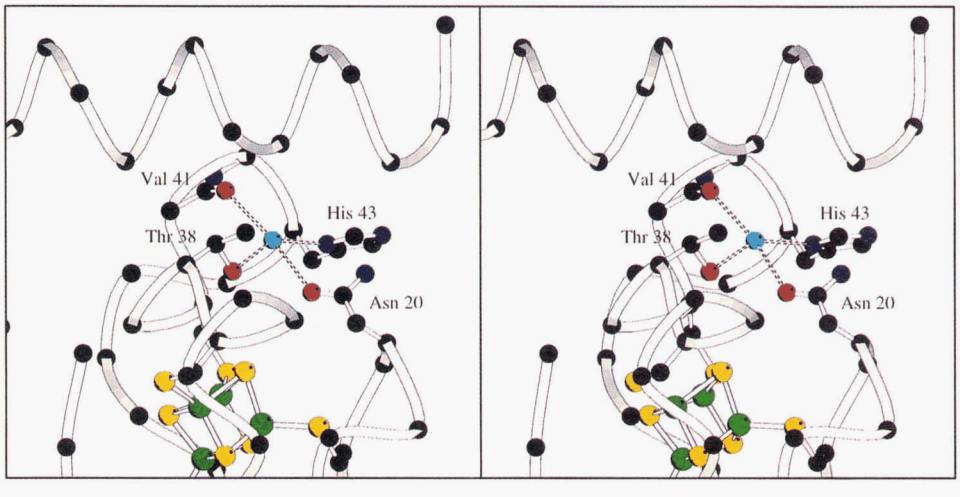

Fig. 6. Stereo view of the single buried water molecule. The C-terminal helix is at the top of the figure and the core of CvFd at the bottom. The four H-bonds between the water molecule and the protein core are shown. Cyan, water oxygen; red, oxygen; blue, nitrogen; yellow, sulfur; green, iron.

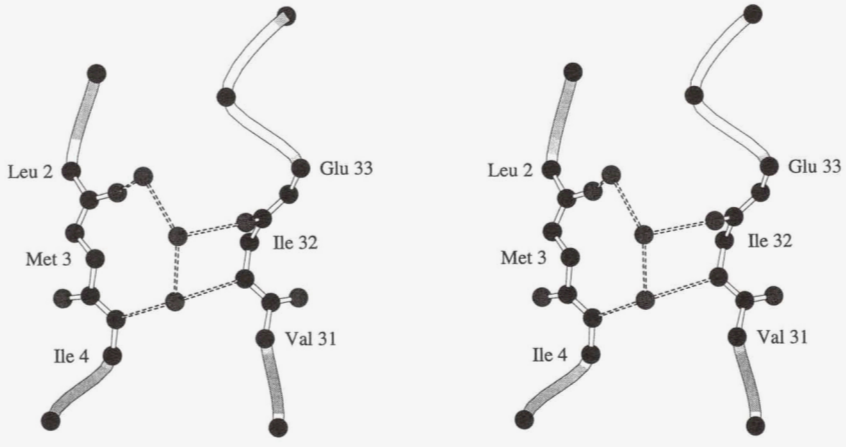

Fig. 7. The "pseudo β-sheet" formed by three water molecules bridging two extended chains of CvFd. There are equivalent waters in CaFd together with a fourth one.

ters is reminiscent of other 2[4Fe-4S] ferredoxins (Adman et al., 1973; Duée et al., 1994). The clusters are buried within the protein core and essentially shielded from the solvent. The geometry of the clusters is compared to that of other ferredoxins below.

The carboxy-terminal residues 69–80 fold into a very regular α-helix with 3.5 turns. This is an original feature, absent in other known ferredoxin structures. The axis of the helix is almost perfectly perpendicular to the axis joining the centers of the two clusters (Fig. 8 and Kinemage 1). As a result of the presence of the helix, CvFd has a somewhat elongated overall shape. This α-helix is linked to the common frame of short ferredoxins by a chain segment encompassing residues 61–67. This includes the exposed Pro 62, causing the segment to bend back and one side of the helix to pack onto the molecular core. Four side chains of the helix, Ile 71, Lys 74, Tyr 75, and Ile 78, interact with a good deal of the coordinating region of Cluster II. Lys 74 plays a key role in orienting the segment connecting the helix to the main body of CvFd and the helix itself (Fig. 9 and Kinemage 1). Indeed, Lys 74 NZ is in a position to establish H-bonds with Pro 34 O, Cys 37 O, one water molecule, and the carboxylate group of Glu 66. The latter is thus bridging Lys 74 and Ala 1 in a stabilizing network of H-bonds (Fig. 9 and Kinemage 1).

Another special feature of CvFd is the extended loop between two of the cysteine ligands of Cluster II (residues 41–48). This region folds in two successive turns around residues 43 and 46 (Fig. 10) preceding the short helix 47–52. The first half of this segment interacts with the terminal α-helix through hydrophobic forces involving Val 41, His 43, Ile 71, and Tyr 75. The ring of Tyr 75 is almost perpendicular to that of His 43, which makes itself a ca. 30° angle with the aromatic ring of Tyr 44. The latter lies on top of the side chain of Gln 48 and contributes to the shielding of Cys 40 from the solvent. This arrangement of three aromatic side chains close to Cluster II is another unique feature of CvFd. The second half of the 41–48 segment is turned toward the exterior of the molecule. For the last two residues (Ser 47-Gln 48), the main chain returns to an orientation very similar to that of CaFd with carbonyl oxygens in a position to form a bifurcated H-bond with the N atom of Glu 51.

The two [4Fe-4S] clusters

In both clusters, the Fe-S bond lengths are very similar. The mean values are 2.21 and 2.20 Å for the bonds within the clusters, and 2.24 and 2.25 Å for the Fe-SG distances (Table 2). The target restraints were 2.23 and 2.27 Å for these two types of Fe-S bonds, respectively. The spread of values, between 2.11 and 2.32 Å within the clusters, and 2.19 to 2.33 Å to the SG atoms, provides no evidence for any significant distortion of the clusters from a more symmetric geometry. Minor deviations may be present but are simply not detected at this resolution. The values are consistent with those reported in other ferredoxins, such as CaFd (Duée et al., 1994). In the latter, the corresponding mean value within the clus-

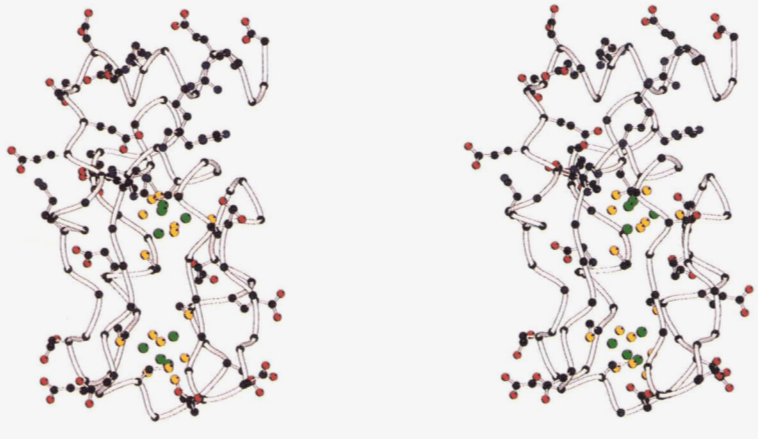

Fig. 8. Ribbon diagram of the CvFd structure including the two [4Fe-4S] clusters. Oxygen atoms of carboxylates are shown in red and nitrogen atoms of basic residues are in blue.

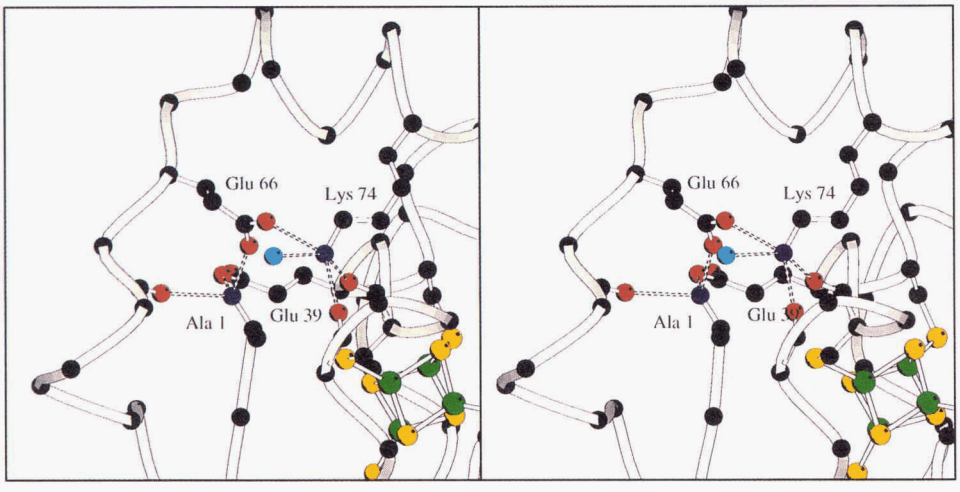

Fig. 9. Stereo view of the H-bond network involving Lys 74 and the N-terminus.

ters is 2.26 Å and 2.25 Å for Fe-SG bonds. Therefore, in view of the apparent similarities of the geometry of the clusters in different ferredoxins, their differing properties are to be explained on the basis of the environment of the clusters rather than differences in their internal geometry. The N-H•••S distances in CvFd can be as long as 3.9 Å (Table 2), which cannot formally classify this length as an H-bond. However, it should be remembered that the coordinate error is estimated at 0.25 Å. In this respect, the network of H-bonds involving the sulfur atoms (S* and SG) of the clusters is conserved between CaFd and CvFd, with one noteworthy exception. Figure 10 shows the cysteine ligands that coordinate the two clusters. The inorganic sulfur S 118 opposite to the Fe 111-SG 18 bond in Cluster II is not in a position to establish an H-bond with Ser 47 NH (equivalent to Gly 41 NH in CaFd) or any other H-bond donor in CvFd; the distance between Ser 47 N and S118 is 5.43 Å. In addition, Cys 40, placed at the beginning of the 41–48 loop, has a different conformation compared to that of the corresponding cysteine in CaFd. Although the CB and SG atoms adopt very similar positions in these proteins and do not change the coordination of the cluster, the relative positions of the CA are 2.20 Å apart (Fig. 10). The change of conformation of Cys 40 is clearly reflected in the values of the torsion angle (Fe-SG 40-CB 40-CA 40) of 45.8° in CvFd and −58.9° in CaFd. This departure of one cluster of CvFd from the very well-conserved H-bond pattern around low-potential clusters in ferredoxins (Backes et al., 1991) is likely to perturb the spin and charge distributions over the cluster and its immediate environment. This is the kind of feature expected to change the redox (Smith & Feinberg, 1990) and electronic (Huber et al., 1995) properties of CvFd compared to other ferredoxins.

Discussion

Comparison to other ferredoxins

The sequences of representative ferredoxins have been aligned using the DALI program (Holm & Sander, 1993) in Figure 11 and Kinemage 2. The algorithm involves superposition of 3D structures, with CvFd as the target model, rather than comparison of sequences.

The core of CvFd most closely resembles the clostridial type ferredoxin represented by CaFd. Many interactions found to participate in the stabilization of CaFd are also present in CvFd. For instance, among the 23 intramolecular H-bonds between main-chain atoms of CaFd, most are conserved between the correspond-

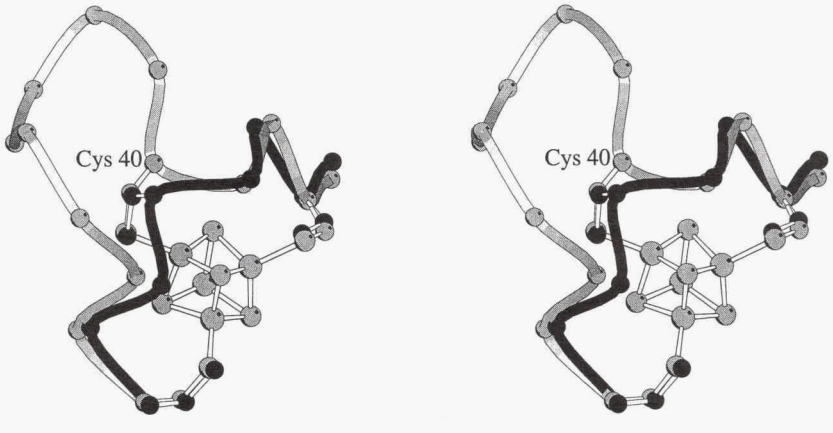

Fig. 10. Stereo view of the region near Cluster II and the external loop. The light chain represents CvFd and the black one CaFd. The CA atoms of Cys 40 in both ferredoxins are separated by 2.20 Å, whereas their side chains overlap very closely.

Table 2. *Bond lengths for the [4Fe-4S] clusters*

Cluster I	(Å)	Cluster II	(Å)
Bonds within the core of the cluster			
Fe 101 S105	2.22	Fe 111 S115	2.17
Fe 101 S106	2.17	Fe 111 S116	2.26
Fe 101 S107	2.21	Fe 111 S117	2.11
Fe 102 S105	2.17	Fe 112 S115	2.25
Fe 102 S106	2.27	Fe 112 S116	2.18
Fe 102 S108	2.18	Fe 112 S118	2.12
Fe 103 S106	2.21	Fe 113 S116	2.15
Fe 103 S107	2.20	Fe 113 S117	2.30
Fe 103 S108	2.32	Fe 113 S118	2.20
Fe 104 S105	2.21	Fe 114 S115	2.15
Fe 104 S107	2.24	Fe 114 S117	2.20
Fe 104 S108	2.17	Fe 114 S118	2.25
Mean	2.21		2.20
Bonds to cysteines			
Fe 101 SG53	2.19	Fe 111 SG18	2.22
Fe 102 SG14	2.30	Fe 112 SG49	2.22
Fe 103 SG8	2.28	Fe 113 SG37	2.36
Fe 104 SG11	2.19	Fe 114 SG40	2.33
Mean	2.24		2.25
N-H···S* distances			
Cys 14 N S105	3.64	Cys 49 N S115	3.64
Ile 9 N S107	3.49	Thr 38 N S117	3.84
Asp 12 N S108	3.62	Ser 47 N S118	No H-bond (5.43)
N-H···SG distances			
Asn 10 N Cys 8 SG	3.59	Glu 39 N Cys 37 SG	3.56
Tyr 30 N Cys 8 SG	3.49	Leu 2 N Cys 37 SG	3.63
Val 13 N Cys 11 SG	3.84	Gly 42 N Cys 40 SG	3.38
Val 55 N Cys 53 SG	3.94	Asn 20 N Cys 18 SG	3.54
Cys 57 N Cys 53 SG	3.79	Ala 22 N Cys 18 SG	3.39

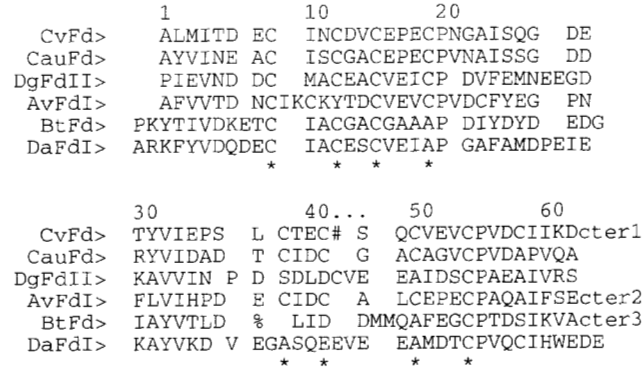

Fig. 11. Structural alignment of [3/4Fe-4S] ferredoxins. Sequences of proteins for which the 3D structure is known were aligned using the DALI program (Holm & Sander, 1993). CvFd was used as the reference structure and the numbering refers to it. Acronyms for the different bacterial species are given in Table 1. Stars give the positions of the cysteines coordinating the Fe-S clusters. Additional parts of sequences are nonhomologous insertions: # = VGHYET and cter1 = PSHEETEDELRAKYERITGEG for CvFd;cter2 = DEVPEDMQEFIQLNAELAEVWPNITEKKDPLPDAEDWD GVKGKLQHLER for AvFdI; % = DNQGIVEVPDI and cter3 = DEPF DGDPNKFE for BtFd.

ing atoms in CvFd; only a few are lost, mainly around Cluster II, but this part of the structure has other stabilizing interactions (see the Results). Thus, the main secondary structure elements of CaFd (and indeed other ferredoxins), namely the two antiparallel β-sheets involving residues (2–5, 52–54) and (22–25, 29–32) and the distorted helical segments joining the clusters, are conserved in CvFd, where β-strands span residues (2–4, 58–60) and (23–25, 30–32). The structures of CaFd and CvFd are superimposed in Figure 12. An approximately Gaussian distribution of discrepancies between the two sets of CA atoms was assumed and pairs were only included if they lay within 2 RMS deviations of one another. The 48 equivalent CA atoms obeying this selection criterion superimpose with an RMS of 0.47 Å. Overall, the structure of the core around the two [4Fe-4S] clusters is very similar in both proteins.

In contrast to the close structural similarity between the inner cores of CaFd and CvFd around the two clusters, the additional extended loop between residues 41 and 47 and the 3.5-turn α-helix at the C-terminus between residues 68 and 79 of CvFd are unique features for which no structural homologue has been found in other ferredoxins. These features are spatially related through a number of interactions in the vicinity of Cluster II, including a network of H-bonds involving Lys 74 (Fig. 9 and Kinemage 1), a cluster of aromatic side chains (His 43, Tyr 44, and Tyr 75), hydrophobic interactions, and a buried water molecule (Fig. 6). Consequently, they determine the coordination mode of the nearby ligands of Cluster II, Cys 37, 40, and 49, and may be the cause of some unusual properties of CvFd.

The six structures of ferredoxins aligned in Figure 11 are shown in comparable orientations in Figure 13. The molecules were superimposed on the basis of the corresponding cluster atoms. A common theme emerging from these 3D structures is the conservation of the folding of the polypeptide chain around the active site(s) for proteins containing one or two [4Fe-4S] clusters. DgFdII is a [3Fe-4S] protein with a backbone fold very similar to those of other short [4Fe-4S] ferredoxins (Kissinger et al., 1991; Fig. 13D). The ferredoxins differ mainly in the C- terminal sequence following the coordination motif of the second cluster if present (Figs. 11, 13 and Kinemage 2). The clostridial type ferredoxins, such as PaFd, CaFd (Fig. 13B), and CpFd, stop a few amino acids after this motif, whereas AvFdI, BtFd, DaFdI, and CvFd have longer C-terminal extensions. However, the folds of these extensions are very different. DaFdI and BtFd (Fig. 13E,F), lacking a second cluster, have three-turn α-helices nearly parallel to the main axis of the protein, which passes through the cluster (and the region where the second cluster would be if there was one). This helix has been proposed to replace the stabilizing effect that is afforded by the second cluster in two-cluster ferredoxins (Fukuyama et al., 1988). In contrast, AvFdI has a bent four-turn α-helix that is not an integral part of the cluster-binding domain (Fig. 13C). The axis of the helix is perpendicular to the axis joining the two clusters and lies approximately midway between them. CvFd provides yet another variation on the theme, with a 3.5-turn helix also perpendicular to the axis joining the two clusters, but lying beyond Cluster II (Fig. 13A).

Evolution of [3/4Fe-4S] ferredoxins

These structural differences are supportive of the divergent evolution of the various ferredoxin families beginning with the duplication of an ancestral gene, as is recognized most easily in short, clostridial type ferredoxins (Otaka & Ooi, 1987). From the presumably oldest sequences retaining an almost perfect internal

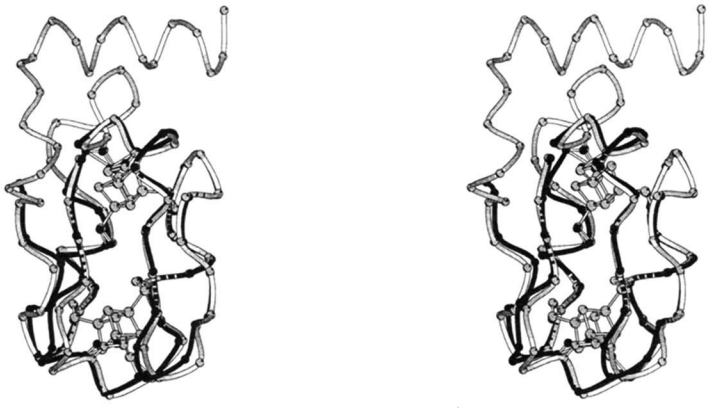

Fig. 12. Structure of CvFd overlapped on over that of CaFd. The light ribbon represents CvFd and the black one CaFd. Only the CvFd clusters are shown as they superimpose on the CaFd pair.

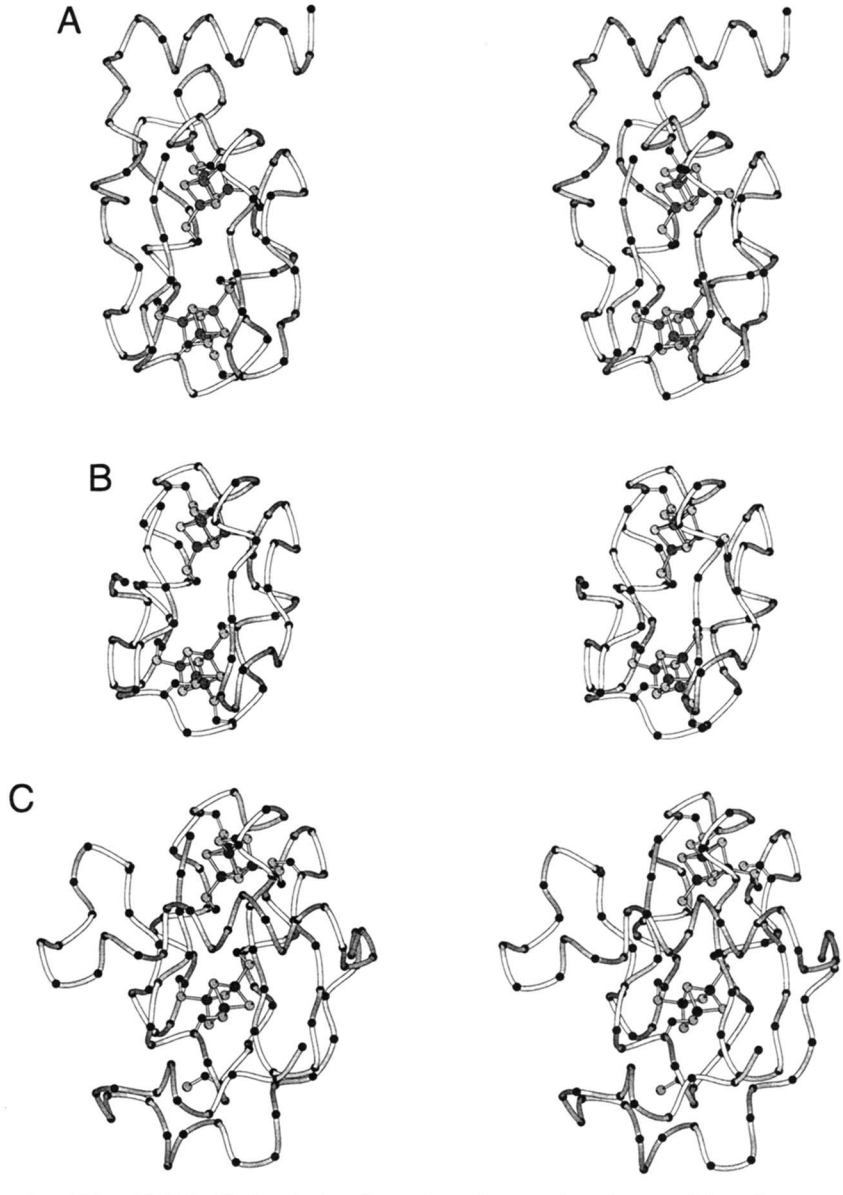

Fig. 13. Representative folds of [3/4Fe-4S] ferredoxins shown in analogous orientations as ribbon diagrams using the program MOLSCRIPT (Kraulis, 1991). **A:** CvFd. **B:** CaFd. **C:** AvFdI. **D:** DgFdII. **E:** DaFdI. **F:** BtFd. Structures of PaFd and CpFd are not shown because they are so similar to that of CaFd. Structures were oriented by superimposing the Fe and S atoms on one or two equivalent clusters. (*Figure continues of facing page.*)

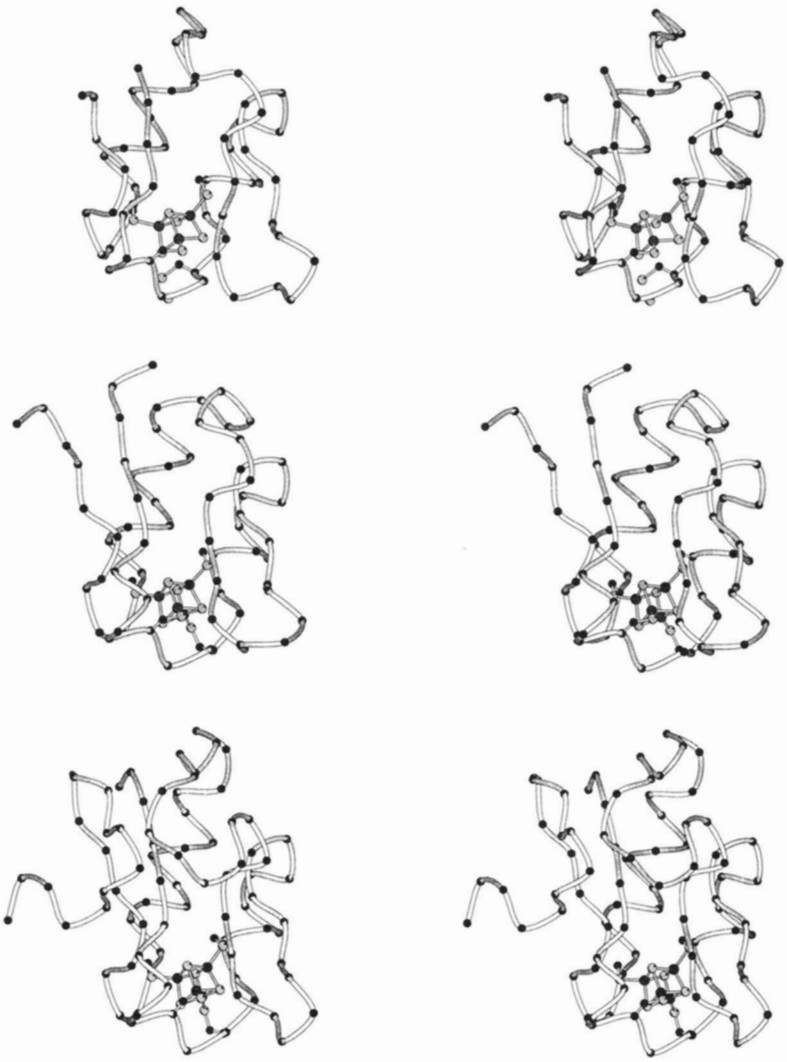

Fig. 13. *Continued.*

symmetry as in CaFd (Figs. 11, 12, 13B and Kinemage 2), several evolutionary events have occurred. One led to the loss of one cluster and its compensation with an α-helix and a C-terminus of variable length (Fukuyama et al., 1988). Indeed, DgFdII, DaFdI, and BtFd (Fig. 13D,E,F) have an almost identical fold over the whole sequence of DgFdII (the shortest of them). Another set of events resulted mainly in the addition of a long C-terminus while retaining both clusters. The latter additions may have occurred independently as witnessed by the lack of sequence homology and by the completely different folding of these regions in CvFd and AvFdI (Fig. 13A,C). In this respect, CvFd appears to be a prototypical protein of a new family, as suggested on other grounds (Moulis, 1996), rather than a member of the subclass of ferredoxins from other photosynthetic bacteria (e.g., Fukuyama et al., 1988).

Mechanistic consequences of Chromatium vinosum ferredoxin structure

The intramolecular electron transfer (ET) rate constant between the clusters of CvFd is at least two, and more probably four, orders of magnitude slower than in CpFd (Huber et al., 1995) and CaFd (unpubl.). Because this reaction occurs at near zero driving force (the reduction potentials of the clusters in a given molecule are almost equal), these differences may arise from different values of the reorganization energy or of the electronic coupling factor in the framework of the current theory of ET reactions (Marcus & Sutin, 1985). A major change in the value of the reorganization energy is not sustained by the close similarity of the folds holding the clusters, including the clusters themselves, in the two types of ferredoxins (Fig. 12), but it cannot be completely ruled out. In these proteins, the clusters are separated by the same distance and the polypeptide environment joining them is almost identical. These properties should therefore lead to similar electronic terms. However, the conformational change of one ligand and the loss of one H-bond on Cluster II in CvFd as compared to CaFd may be responsible for the differences in the electronic structures of the clusters, as witnessed by EPR spectra (Gaillard et al., 1993; Huber et al., 1995). Such features are expected to contribute to the electronic coupling between the redox centers and their effects will be better evaluated by studies at higher resolution and the determi-

nation of their structural and functional influences in site-directed mutated forms of these ferredoxins, both in solution and in the crystal.

Materials and methods

C. vinosum ferredoxin was purified as described previously (Huber et al., 1995). The UV-visible spectrum of this material gave purity criteria indicative of homogenous ferredoxin (Bachofen & Arnon, 1966).

Crystallization

Crystals of CvFd were obtained several years ago, but due to their hollow shape were not suitable for structure analysis (Bachofen & Arnon, 1966; Sieker, 1988). The original crystallization experiments were performed by vapor equilibration using hanging drop and sitting drop techniques. The hanging drop technique tended to produce long hollow hexagonal prisms (tubes), as mentioned above, whether performed at 22 °C or at 8 °C. Some drops contained thick but small rectangular plates that would often dissolve as long hexagonal prisms began to develop. None of these crystals were large enough for diffraction studies.

Subsequent crystallization experiments, under more rigorous control, produced nice dark brown crystals of CvFd useful for diffraction studies. In order to reduce the rate of crystal growth and prevent development of the hollow end in the prisms, vapor equilibration was slowed down by using the sitting drop technique in a petri dish at 8 °C. Several drops with larger volumes were set up in the dish to enhance the probability of getting larger crystals, not only by increasing the total amount of protein, but also by slowing the relative rate of vapor exchange. The vapor exchange cavity was filled with argon to reduce the possibility of protein denaturation by molecular oxygen. The sitting drops consisted of 25 μL of protein solution and 25 μL of reservoir solution.

The 5-mL reservoir solution was 70% saturated ammonium sulfate (2.9 M), 100 mM NaCl buffered with 100 mM Tris-maleate at pH 6.5. The addition of 100 mM NaCl seemed to help crystal development, but there was no clear indication of shifting the crystal growth to plates or hexagonal prisms. Fortunately, some long hexagonal prisms grew large enough without the development of hollow ends for diffraction studies.

Data collection

Diffraction data were collected from a single crystal with dimensions about 0.3 × 0.3 × 0.7 mm, mounted in a thin-walled glass capillary with its *c*-axis approximately along the spindle. Data were collected on the EMBL Hamburg synchrotron beam line X31 at DESY. A MAR Research 180-mm imaging plate scanner was used as a detector. The wavelength was set to 0.92 Å. Two sets of data were recorded, one with a 10 times shorter exposure time than the other, in order to record properly the strong low-resolution intensities and weaker high-resolution reflections, respectively. For a crystal with point group symmetry 32 rotated around the *c*-axis, it is sufficient to cover 30° of total rotation between the directions *a* and *a** for a complete data set. Misorientation by 9° of the crystal *c*-axis from the spindle alleviated the effect of the blind region, ensuring high data completeness.

Images were processed and intensities integrated with the HKL program suite (Otwinowski & Minor, 1994). The symmetry of the crystal was confirmed to be $P3_121$ or $P3_221$ (indistinguishable by diffraction)—the presence of the threefold screw axis was clear from the absence of 00l reflections with $l \neq 3n$. Cell dimensions were $a = 52.0$, $c = 77.2$ Å. The data were 97% complete. The overall $R(I)$ merge of 8.1% ranged from 4.3% at low resolution to more than 35% in the highest-resolution shell, the latter giving a clear indication that 2.1 Å was the real diffraction limit of the crystal. Moreover, the crystal mosaicity refined to 1°, again suggesting significant imperfection.

Molecular replacement

The program AMoRe (Navaza, 1993) was used for molecular replacement. As a search model, the coordinates of PaFd were used (PDB entry 1FDX, Table 1). This model, refined at 2.0 Å resolution, is only about 2/3 of the CvFd peptide chain but, due to the presence of the two heavy [4Fe-4S] clusters, it constitutes much more in terms of scattering power.

PaFd ferredoxin is ellipsoidal, with largest and smallest axes of 26 and 20 Å. The rotation function was solved using data in the resolution range 3–10 Å and a maximum Patterson vector integration range of 15 Å. Several significant peaks occurred in the rotation function, of which two gave much higher correlation coefficients and lower *R*-factors than the others after the translation function search and subsequent rigid-body fitting when space group $P3_121$ was assumed. No prominent peaks were observed for space group $P3_221$. One peak with high correlation coefficient corresponds to the correct solution, the other relates to the solution with the two [4Fe-4S] clusters interchanged, due to the internal symmetry of the PaFd molecule.

Refinement

The starting model from molecular replacement was subjected to an automated refinement procedure (ARP; Lamzin & Wilson, 1993) with automatic building of solvent and a bulk solvent correction applied. This utilized PROLSQ (Konnert & Hendrickson, 1980) and other programs from the CCP4 suite (CCP4, 1994). Steps of ARP were interspersed with inspection of electron density maps and manual rebuilding of the polypeptide chain using the program FRODO (Jones, 1978). The correct side chains and missing parts of the main chain gradually appeared. There was no electron density for the two C-terminal residues expected from the sequence; they are presumed to be disordered and are not included in the model.

The conventional restraints were applied to the polypeptide chain (Engh & Huber, 1991). The Fe-S distances were weakly restrained to targets of 2.23 Å for bonds within the cluster and 2.27 Å for bonds to cysteine sulfur atoms. These were the average values obtained during an attempt to refine the clusters anisotropically with the program SHELXL with common distance restraints (Sheldrick & Schneider, 1996). The final model consists of 80 amino acid residues (612 protein atoms), 2 [4Fe-4S] clusters, and 85 water molecules. All 80 residues were built with a single conformation. The final *R*-factor is 19.2% for all data within the 20–2.1 Å range. No σ cut-off was applied to the X-ray amplitudes during refinement. A rough estimate of the mean coordinate error can be obtained from the σ_A plot (Read, 1986) as 0.25 Å.

Supplementary material in Electronic Appendix

The merging $R(I)$ factor for symmetry related reflections, $R = \Sigma|I - \langle I\rangle|\Sigma I$, and the *R*-factor for the final model are plotted as a

function of resolution. Tables containing the data collection summary, the results of molecular replacement, and the summary of refinement and characteristics of the model are available.

Acknowledgments

J.-M.M. thanks Drs. P. Kyritsis and J. Meyer for discussions and careful reading of the manuscript.

References

Adman ET, Sieker LC, Jensen LH. 1973. The structure of a bacterial ferredoxin. *J Biol Chem 248*:3987–3996.

Adman ET, Sieker LC, Jensen LH. 1976. Structure of *Peptococcus aerogenes* ferredoxin. Refinement at 2 Å resolution. *J Biol Chem 251*:3801–3806.

Bachofen R, Arnon DI. 1966. Crystalline ferredoxin from the photosynthetic bacterium *Chromatium*. *Biochim Biophys Acta 120*:259–265.

Backes G, Mino Y, Loehr TM, Meyer TE, Cusanovich MA, Sweeney WV, Adman ET, Sanders-Loehr J. 1991. The environment of Fe_4S_4 clusters in ferredoxins and high-potential iron proteins. New information from X-ray crystallography and resonance Raman spectroscopy. *J Am Chem Soc 113*:2055–2064.

Bernstein FC, Koetzle TF, Williams GJB, Meyer EF Jr, Brice MD, Rodgers JR, Kennard O, Simanouchi T, Tasumi M. 1977. The Protein Data Bank: A computer-based archival file for macromolecular structures. *J Mol Biol 112*:535–542.

Bertini I, Donaire A, Feinberg BA, Luchinat C, Piccioli M, Yuan H. 1995. Solution structure of the oxidised 2[4Fe-4S] ferredoxin from *Clostridium pasteurianum*. *Eur J Biochem 232*:192–205.

Cammack R. 1992. Iron clusters in enzymes. *Adv Inorg Chem 38*:281–322.

Carter CW Jr, Kraut J, Freer ST, Xuong N, Alden RA, Sieker LC, Adman ET, Jensen LH. 1972. A comparison of Fe_4S_4* clusters in high-potential iron protein and in ferredoxin. *Proc Natl Acad Sci USA 69*:3526–3529.

CCP4. 1994. Collaborative Computational Project, Number 4. The CCP4 suite: Programs for protein crystallography. *Acta Crystallogr D 50*:760–763.

Duée ED, Fanchon E, Vicat J, Sieker LC, Meyer J, Moulis JM. 1994. Refined crystal structure of the 2[4Fe-4S] ferredoxin from *Clostridium acidurici* at 1.84 Å resolution. *J Mol Biol 243*:683–695.

Engh RA, Huber R. 1991. Accurate bond and angle parameters for X-ray protein structure refinement. *Acta Crystallogr A 47*:392–400.

Fukuyama K, Matsubara H, Tsukihara T, Katsube Y. 1989. Structure of [4Fe-4S] ferredoxin from *Bacillus thermoproteolyticus* refined at 2.3 Å resolution. *J Mol Biol 210*:383–398.

Fukuyama K, Nagahara Y, Tsukihara T, Katsube Y, Hase T, Matsubara H. 1988. Tertiary structure of *Bacillus thermoproteolyticus* [4Fe-4S] ferredoxin. Evolutionary implications for bacterial ferredoxins. *J Mol Biol 199*:183–193.

Gaillard J, Quinkal I, Moulis JM. 1993. Effect of replacing conserved proline residues on the EPR and NMR properties of *Clostridium pasteurianum* 2[4Fe-4S] ferredoxin. *Biochemistry 32*:9881–9887.

Holm L, Sander C. 1993. Protein structure comparison by alignment of distance matrices. *J Mol Biol 233*:123–138.

Huber JG, Gaillard J, Moulis JM. 1995. NMR of *Chromatium vinosum* ferredoxin: Evidence for structural inequivalence and impeded electron transfer between the two [4Fe-4S] clusters. *Biochemistry 34*:194–205.

Jones TA. 1978. A graphics model building and refinement system for macromolecules. *J Appl Crystallogr 11*:268–272.

Kissinger CR, Sieker LC, Adman ET, Jensen LH. 1991. Refined crystal structure of ferredoxin II from *Desulfovibrio gigas* at 1.7 Å. *J Mol Biol 219*:693–715.

Konnert JH, Hendrickson WA. 1980. A restrained-parameter thermal-factor refinement procedure. *Acta Crystallogr A 36*:344–350.

Kraulis PJ. 1991. MOLSCRIPT: A program to produce both detailed and schematic plots of protein structures. *J Appl Crystallogr 24*:946–950.

Lamzin VS, Wilson KS. 1993. Automated refinement of protein models. *Acta Crystallogr D 49*:129–147.

Laskowski RA, MacArthur MW, Moss DS, Thornton JM. 1993. PROCHECK: A program to check the stereochemical quality of protein structures. *J Appl Crystallogr 26*:283–291.

Marcus RA, Sutin N. 1985. Electron transfers in chemistry and biology. *Biochim Biophys Acta 811*:265–322.

Matsubara H, Saeki K. 1992. Structural and functional diversity of ferredoxins and related proteins. *Adv Inorg Chem 38*:223–280.

Matthews BW. 1968. Solvent content of protein crystals. *J Mol Biol 33*:491–497.

Moulis JM. 1996. Molecular cloning and expression of the gene encoding *Chromatium vinosum* 2[4Fe-4S] ferredoxin. *Biochim Biophys Acta*. Forthcoming.

Moulis JM, Davasse V. 1995. Probing the role of electrostatic forces in the interaction of *Clostridium pasteurianum* ferredoxin with its redox partners. *Biochemistry 34*:16781–16788.

Moulis JM, Lutz M, Gaillard J, Noodleman L. 1988. Characterization of $[4Fe\text{-}4Se]^{2+/3+}$ high-potential iron–sulfur protein from *Chromatium vinosum*. *Biochemistry 27*:8712–8719.

Navaza J. 1994. AMoRe: An automated package for molecular replacement. *Acta Crystallogr A 50*:157–163.

Otaka E, Ooi T. 1987. Examination of protein sequence homologies: IV. Twenty seven bacterial ferredoxins. *J Mol Evol 26*:257–267.

Otwinowski Z, Minor W. 1994. *DENZO: A film processing program for macromolecular crystallography*. New Haven, Connecticut: Yale University.

Pétillot Y, Forest E, Meyer J, Moulis JM. 1995. Observation of holoprotein molecular ions of several ferredoxins by electrospray-ionization mass spectrometry. *Anal Biochem 228*:56–63.

Read RJ. 1986. Improved Fourier coefficients for maps using phases from partial structures with errors. *Acta Crystallogr A 42*:140–149.

Séry A, Housset D, Serre L, Bonicel J, Hatchikian C, Frey M, Roth M. 1994. Crystal structure of the ferredoxin I from *Desulfovibrio africanus* at 2.3 Å resolution. *Biochemistry 33*:15408–15417.

Sheldrick GM, Schneider TR. 1996. SHELXL: High-resolution refinement. *Methods Enzymol*. Forthcoming.

Sieker LC. 1988. Interesting observations on the nature of protein crystals and their growth. *J Crystal Growth 90*:31–38.

Smith ET, Feinberg BA. 1990. Redox properties of several bacterial ferredoxins using square wave voltammetry. *J Biol Chem 265*:14371–14376.

Stout CD. 1989. Refinement of the 7 Fe ferredoxin from *Azotobacter vinelandii* at 1.9 Å resolution. *J Mol Biol 205*:545–555.

Wilson AJC. 1942. Determination of absolute from relative X-ray data intensities. *Nature (Lond) 150*:151–152.